Envelope Spectrum Analysis With Algorithm Simulations To Detect Railway Wheel Out-of-roundness Defects

Vítor Gonçalves[1], Araliya Mosleh[1], Cecília Vale[1], Pedro A. Montenegro[1]

[1]*Department of Civil Engineering, Faculty of Engineering, University of Porto*
Rua Dr. Roberto Frias, 4200-465, Porto, Portugal
vtgoncalves@fe.up.pt, amosleh@fe.up.pt, cvale@fe.up.pt, paires@fe.up.pt

Abstract. The objective of this work is to identify defects in railway vehicle wheels using an envelope spectrum analysis technique combined with spectral kurtosis analysis. The analysis is performed on data collected by a simulated wayside monitoring system situated on the track. A dynamic 3D interaction model is implemented using the in-house software VSI-Vehicle-Structure Interaction Analysis to simulate the dynamic interactions between a passing train and the track. In this work, an *Alfa Pendular* passenger vehicle and a section of the Portuguese Northern Line serve as the basis for the numerical models of the train and track, respectively. In the simulations, three types of wheel flat profiles and three periodic polygonal wheel profiles are analysed, along with results obtained from dynamic analyses conducted on wheels that do not exhibit any type of damage. Additionally, the simulation considers track irregularity profiles generated based on the Federal Railroad Administration (FRA) standards. The dynamic responses of several strain gauges and accelerometer sensors located on the rail between sleepers are then evaluated through numerical calculations. To further validate the methodology, the influence of different train speeds, track unevenness profiles, and wheel fault severity are considered. For validation purposes, the right wheel of the first wheelset is modelled with a defect, but the detection methodology is effective for damaged wheels modelled in any position. The application of the methodology demonstrates that envelope spectrum analysis can successfully differentiate between healthy and defective wheels.

Keywords: algorithm, numerical simulations, wheel out-of-roundness, wheel flat, polygonised wheel.

1 Introduction

The growing demand for railway transportation, with increased axle loads, presents challenges for train wheels, including operational disruptions, higher operational and maintenance costs, infrastructure deterioration, and, in severe instances, the risk of train derailments. Railway operators are responding with advanced maintenance efforts to swiftly identify defects, aiming to cut long-term expenses, enhance safety, and uphold overall rail operations stability.

There are two main categories for detecting wheel defects: onboard monitoring systems (Bernal et al. [1] and Bosso et al. [2]) and wayside monitoring systems (Pintão et al. [3] and Pimentel et al. [4]). Wayside monitoring systems are preferred over onboard monitoring systems for wheel defect detection, enabling the analysis of all wheels' conditions as trains pass by (Meixedo et al. [9], Amini et al. [10], Colaço et al. [11], Mosleh et al. [12-14], Kouroussis et al. [15] and Alexandrou et al. [16]).

Several methods have been researched for detecting wheel detect out-of-roundness (OOR) defects in railway vehicles, such as the works of the author in Mosleh et al. [17-19] and the work of Wang et al. [20] for wheel flat detection, and Xu et al. [21] and Fang et al. [22] for polygonal wheel detection. The objective of this work lies in implementing envelope spectrum analysis with a wayside monitoring system to distinguish between a defective wheel and a healthy one, considering defects with high impact frequency (wheel flats) as well as smaller defects around the wheel (polygonization). Furthermore, the study analyses the impact of track irregularity, train speed, and defect severity on the detection of the damaged wheel. The study focuses on the dynamic responses of sensors placed on the rail, between the sleepers, and specifically targets the right wheel of the first wheelset.

2 Defect detection methodology

As mentioned earlier, the detection methodology implements envelope spectrum analysis. Envelope spectrum analysis involves a complex demodulation procedure in which each frequency is shifted to zero and subsequently subjected to a low-pass filter (Hasan [23]). Spectral kurtosis (SK) is used to demodulate the band section of the envelope analysis, providing a similar indication of the band being demodulated without the need for historical data. To compute the SK of a signal, the main signal is divided into different frequency bands, obtaining the kurtosis of each frequency band (Antoni [24]).

Figure 1 illustrates the procedure for detecting a damaged wheel. The process included two main blocks. The first block of the flowchart, inside the orange dotted box, refers to the calculation of the envelope spectrum. For each sensor, a time-series signal, $R_i(t)$, is recorded, as shear or acceleration. By determining the kurtogram of the signal, the level of the coefficient series, l, and the number of filters, i, applied at level l, are determined, which are used to calculate the bandwidth frequency, Δf (eq. (1)), with a sampling frequency, F_s, of 10,000 Hz, and the centre frequency, f_0 (eq.(2)). The signal is then demodulated by multiplying it with a factor, $X(t)$, and, by applying a low-pass filter, the envelope spectrum is calculated. The procedure is then repeated until all sensors are analysed.

$$\Delta f = 2^{(-l-1)} F_S. \tag{1}$$

$$f_0 = (i + 0.5)\Delta f. \tag{2}$$

The second block of the flowchart, inside the green dotted box, shows the detection phase of the methodology. Two criteria are used to detect a damaged wheel: (a) a lag between the signal of each sensor, or (b) the envelope spectrum amplitude difference for a defective wheel and a healthy wheel. When all sensor responses align, it indicates the passing of a healthy wheel. Otherwise, when noticeable amplitude delays in the envelope spectrum are observed, it indicates the presence of a defective wheel. Additionally, envelope spectrum amplitudes of healthy wheels are considerably lower than the ones seen on damaged ones.

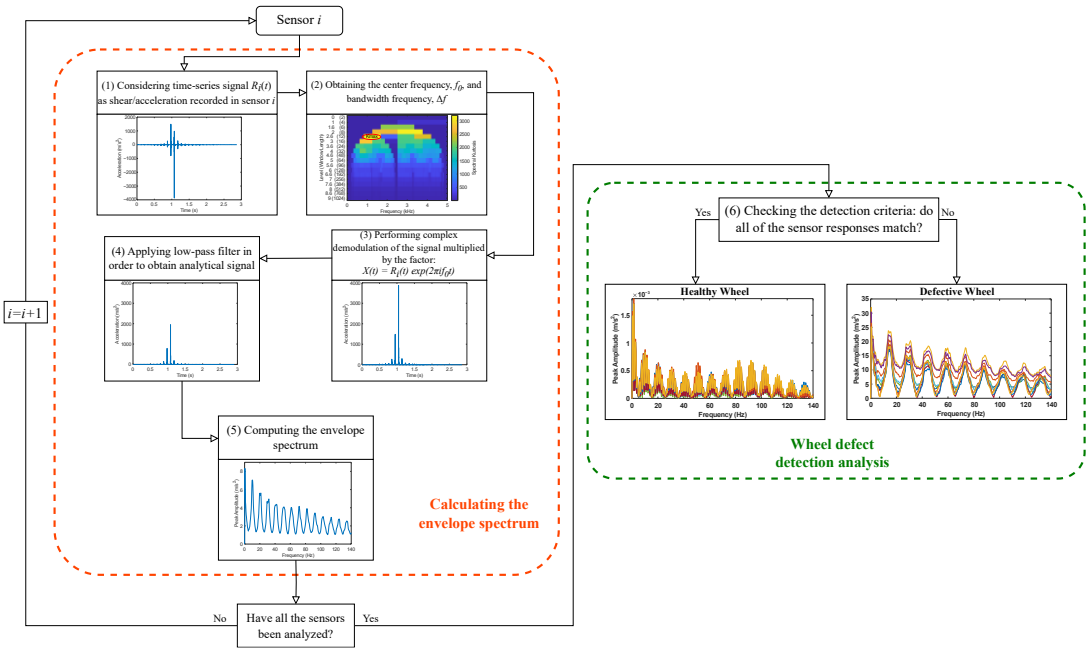

Figure 1. Wheel defect detection methodology flowchart

3 Numerical Modelling

In this research, the wayside condition monitoring system is comprised of 10 accelerometers and 10 strain gauges (SGs) positioned on the rail. Two distinct sensor arrangements are examined, seen in Fig. 2. Positions 1 to 10 (red dots inside black box) are indicated by either SGs (layout 1, green dots) or accelerometers (layout 2, blue dots) mounted on the rail between sleepers. The intention is to assess the track response using different sensors by

positioning both SGs and accelerometers at the same location for comparison purposes.

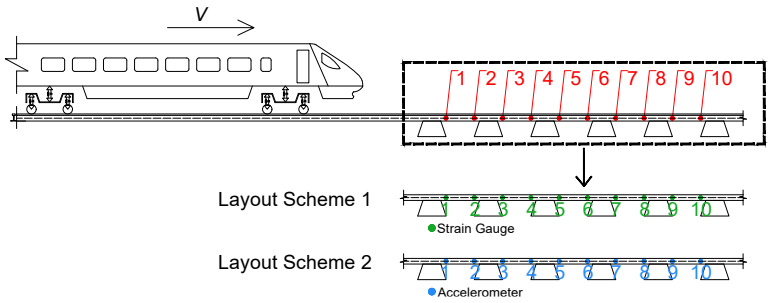

Figure 2. Layout of the wayside monitoring system. Adapted from Gonçalves et al. [25]

This study analyses six defective wheels: three different severities of wheel flats and three different periodic polygonal wheels. During analysis, the defective wheel corresponds to the right wheel of the first wheelset. Table 1 depicts the characteristics of the defective wheels implemented in this work. The profiles are added as periodic wheel irregularities in the software MATLAB® [26]. The authors detail in Gonçalves et al. [25] how the wheel flat and polygonal wheel profiles are generated.

Table 1. Wheel flat and polygonization profiles

Flat profile nomenclature	Flat length (L) [mm]	Flat depth (D) [mm]
wf1	20	0.058
wf2	80	0.930
wf3	140	2.800
Polygonised profile nomenclature	**Harmonic order (θ)**	**Reasoning**
wp1	5	Detected in operational services (Tao et al. [27])
wp2	12	Intermediate value
wp3	20	Highest harmonic possible for the wheel circumference (Johansson and Andersson [28])

The train is modelled after an *Alfa Pendular* Portuguese passenger train. The characteristics of the vehicle are captured through a model created with ANSYS® [29]. Rigid beam finite elements are used to model the various components of the train, encompassing the carbody, bogies, and wheelsets. For accurate representation, these components are assigned mass elements to simulate their mass and rotational inertia. Additionally, spring-dampers are integrated into the model to simulate the behaviour of suspensions.

The numerical model of the track is based on a track section of the Portuguese Northern Line using ANSYS® [29]. The model employs linear finite elements and is structured with three layers to emulate the various components of the track: ballast, sleeper, and rail. These elements are interconnected through spring-dampers, which simulate the behaviour of the ballast and fastener pads as described by the author's previous work in Mosleh et al. [18]. The track irregularity profiles are generated according to a stationary stochastic process derived from a power spectral density function derived from Fries and Coffey [30] and Hamid and Yang [31], which relate to track quality according to the Federal Railroad Administration (FRA). They are added as constraint equations in MATLAB® [26]. In the numerical simulations, two track profiles are considered: "class 6" being the least severe according to the FRA, and "class 7", generated profile from real measurements taken from an inspection vehicle in the Portuguese Northern Line. The authors provide further details regarding the track irregularity profile creation in Gonçalves et al. [25].

Simulations of train-track interactions utilize the in-house VSI – Vehicle-Structure Interaction software. Initially devised by Neves et al. [32] and the author's previous work in Montenegro et al. [33] to address vertical interaction, it was expanded by the author in Montenegro et al. [34] to include lateral dynamics. This integration is made possible through a validated wheel-rail contact model (Montenegro et al. [34]), built on a specialized contact finite element. The element comprises three key steps: (a) determining contact points using nonlinear equations; (b) calculating normal forces with Hertz theory and (c) computing creep forces due to rolling friction

using the USETAB routine (Kalker et al. [35]), which pre-computes longitudinal and lateral forces stored in a lookup table for interpolation during dynamic analysis based on creepages and Hertz contact ellipse semi-axes ratio. The unified system, comprising unknown displacements and contact forces, is solved directly using an optimized block factorization algorithm (Montenegro et al. [34]). This numerical approach, rooted in the finite element method, accommodates intricate structures and vehicles. The tool is implemented in MATLAB® [26], utilizing structural matrix data from vehicles and tracks previously modelled in ANSYS® [29]. Further insights into the train-track interaction tool, as well as the wheel-rail contact model and their validation, are provided by the author's previous work in Montenegro et al. [34].

4 Results for wheel defect detection

4.1 Wheel flat detection

Figure 3 shows the envelope spectrum measure from the accelerometers regarding one wheel flat profile under various circumstances. Comparing Fig. 3 **(a)** and Fig. 3 **(b)**, no significant difference can be detected, showing that the irregularity profile of the track does not influence the detection methodology. Nonetheless, a lag in the sensor signals can be found, showing the presence of a defective wheel. When analysing different train speeds, V, as seen between Fig. 3 **(b)** and Fig. 3 **(c)**, the peak amplitude of the envelope spectrum signal increases with speed, as well as the defect frequency, d_f (eq. (3)), revealing that the methodology is sensible to the travel speed of the train. The same conclusions can be seen when analysing the envelope spectrum analysis made using the SGs (Fig. 4).

$$d_f = \frac{V}{(2\pi r_w)}. \tag{3}$$

Figure 5 shows the effect of different severities of wheel flats measured with accelerometers. Comparing Fig. 5 **(a)** and Fig. 5 **(b)**, more severe flats lead to higher peak amplitude of the envelope spectrum, demonstrating the sensitivity of the methodology to different severities of wheel flat. The difference in peak amplitude is significantly noticeable when comparing the damage scenarios to a healthy wheel scenario (Fig. 5 **(c)**), as expected from the methodology.

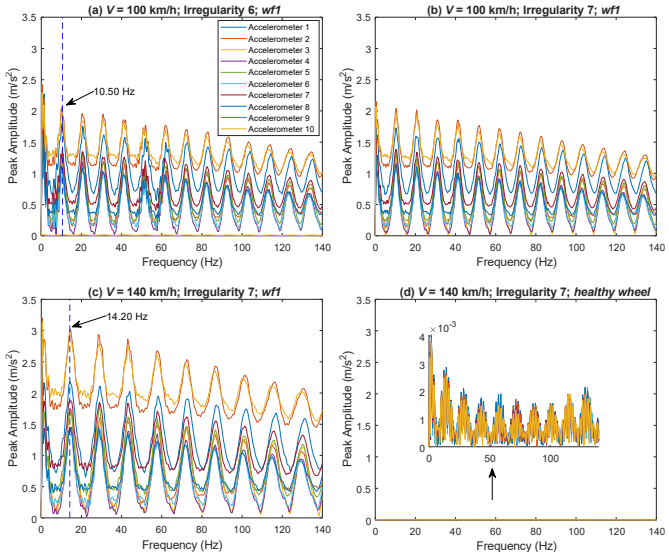

Figure 3. Accelerometers: **(a,b)** effect of different track profiles; **(b,c)** effect of different train speeds; **(d)** healthy wheel. The dotted vertical line indicates the defect frequency (eq. (3))

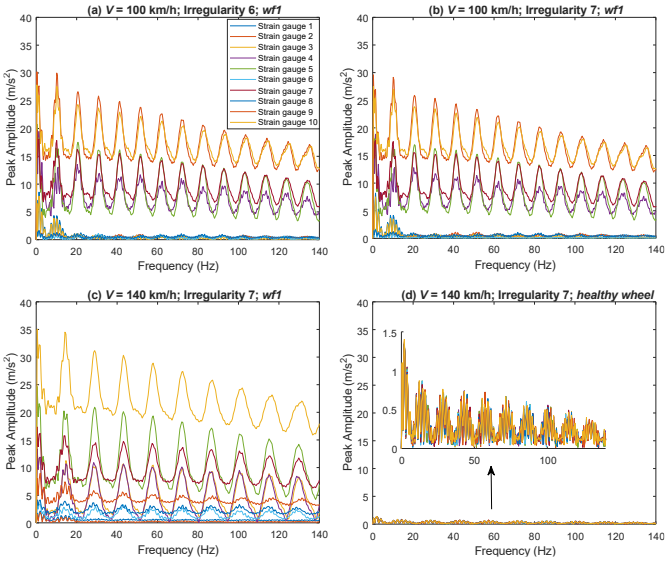

Figure 4. SGs: **(a,b)** effect of different track profiles; **(b,c)** effect of different train speeds; **(d)** healthy wheel

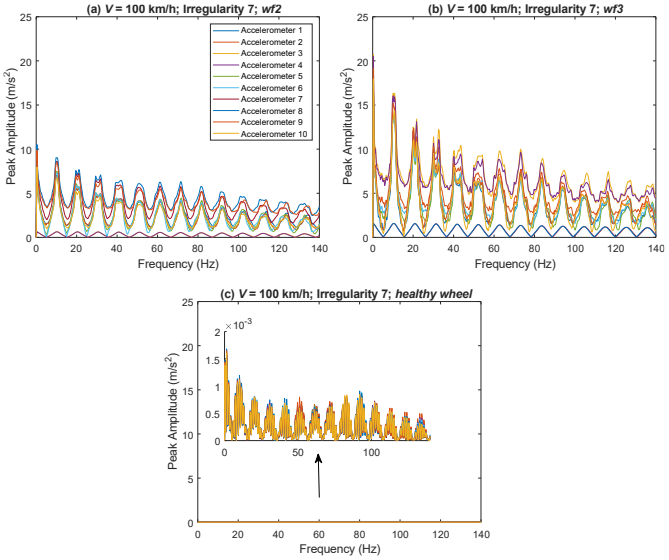

Figure 5. Accelerometers: **(a,b)** effect of different flat severities; **(c)** healthy wheel

4.2 Polygonal wheel detection

Figure 6 shows the envelope spectrum measure from the accelerometers regarding one polygonized wheel profile under various circumstances. As with wheel flats, no significant difference can be detected for different track unevenness profiles (Fig. 6 **(a)** and Fig.6 **(b)**), while still showing a lag in the sensor signals. Train speed does influence the envelope spectrum results, as higher speeds generate higher peak amplitude signals for the envelope spectrum (Fig. 6 **(b)** and Fig.6 **(c)**), similar to what can be observed with wheel flats. When analysing the results from the SGs (Fig. 7), it becomes impossible to distinguish a polygonized wheel from a healthy one.

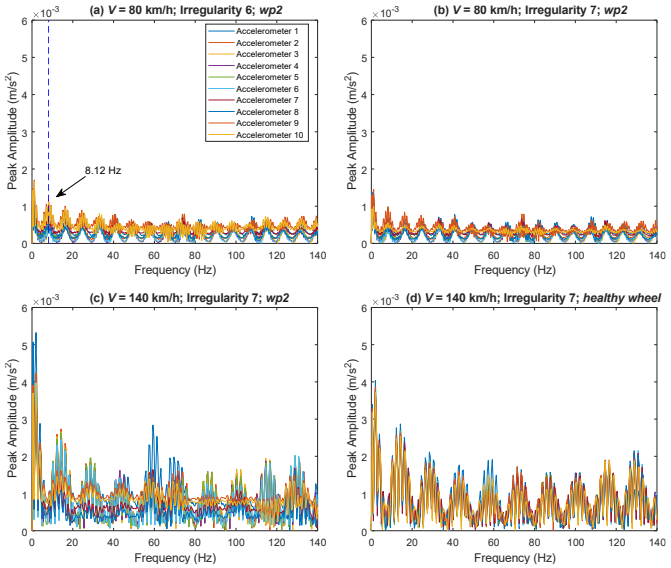

Figure 6. Accelerometers: **(a,b)** effect of different track profiles; **(b,c)** effect of different train speeds; **(d)** healthy wheel. The dotted vertical line indicates the defect frequency (eq. (3))

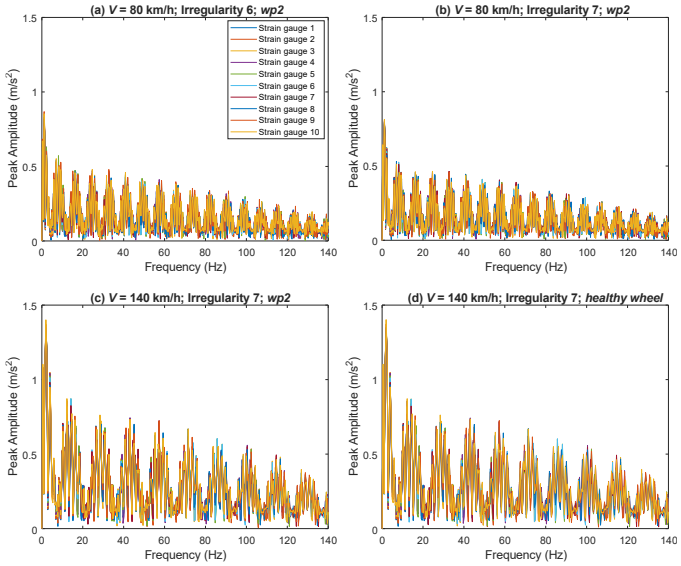

Figure 7. SGs: **(a,b)** effect of different track profiles; **(b,c)** effect of different train speeds; **(d)** healthy wheel

Figure 8 shows the effect of different harmonic orders for wheel polygonization measured with accelerometers. Comparing Fig. 8 **(a)** and Fig. 8 **(b)**, higher harmonic orders for polygonal wheels show higher peak amplitude values of the envelope spectrum, as well as increasing the lag between the signals of each sensor. The difference in peak amplitude is much less noticeable when comparing the damage scenarios to a healthy wheel scenario (Fig. 8 **(c)**) compared to the wheel flat analyses, being almost identical for lower harmonic orders of polygonal wheels (Fig. 8 **(a)** and Fig. 8 **(c)**).

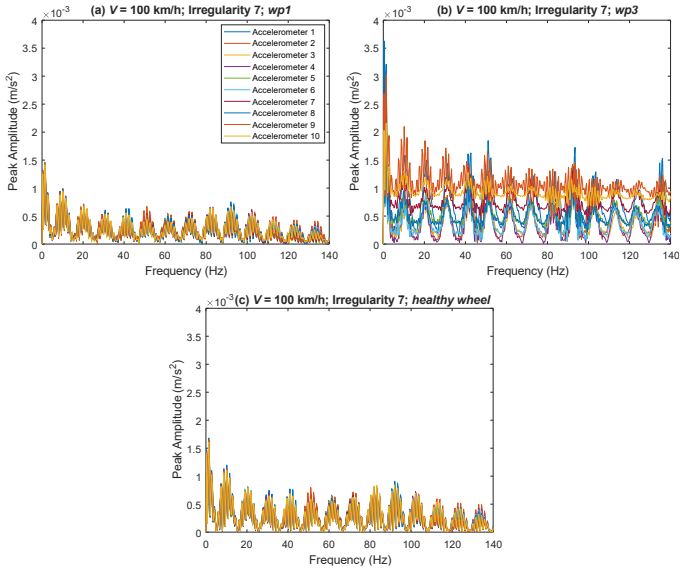

Figure 8. Accelerometers: **(a,b)** effect of different harmonic orders for polygonization; **(c)** healthy wheel

5 Conclusions

The main achievements from the study presented in this paper are summarized as follows:

- The methodology showcased here exhibits the ability to detect wheel flats under different conditions of track unevenness, train speeds, and flat severities. This is achieved by employing both accelerometers and SGs;
- A flat is detected by a lag in signal response and high peak amplitude values of the envelope spectrum;
- The process of detection is accomplished by taking into account various track irregularity profiles, train speeds, and harmonic orders for polygonised wheels. The detection of this particular type of wheel defect can only be accomplished using accelerometers;
- The sole indicator for detecting wheel polygonization is the lag in the signal response;
- The detection of wheel defects remains unimpacted by track irregularities. However, the methodology's ability to detect defects is amplified by higher train speeds and more pronounced detective wheels.

The results achieved through the application of the methodology showcase the effective distinction between a healthy wheel and a defective one using envelope spectrum analysis. To enhance the method, incorporating deep learning algorithms offers a productive way to identify wheel defects using sensor data or envelope spectrum, as well as validating the approach presented in real-world situations.

Acknowledgements. We gratefully appreciate the financial support from the Base Funding-UIDB/04708/2020and Programmatic Funding-UIDP/04708/2020 of the CONSTRUCT—Instituto de Estruturas e Construções, funded by national funds through the FCT/MCTES (PIDDAC). The paper reflects research developed in the ambit of the project Way4SafeRail, NORTE-01-0247-FEDER-069595, founded by Agência Nacional de Inovação S.A., program P2020|COMPETE—Projetos em Copromoção. Moreover, the second author acknowledges Grant no. 2021.04272.CEECIND from the Stimulus of Scientific Employment, Individual Support (CEECIND)—4th Edition provided by FCT—Fundação para a Ciência e Tecnologia.

Authorship statement. The authors hereby confirm that they are the sole liable persons responsible for the authorship of this work, and that all material that has been herein included as part of the present paper is either the property (and authorship) of the authors, or has the permission of the owners to be included here.

References

[1] E. Bernal, M. Spiryagin, and C. Cole. Onboard condition monitoring sensors, systems and techniques for freight railway vehicles: A review. *IEEE Sensors Journal*, vol. 19, n. 1, pp. 4–24, 2019.
[2] N. Bosso, A. Gugliotta, M. Magelli, and N. Zampieri. Monitoring of railway freight vehicles using onboard systems. *Procedia Structural Integrity*, vol. 24, pp. 692–705. AIAS 2019 International Conference on Stress Analysis, 2019.
[3] B. Pintão, A. Mosleh, C. Vale, P. Montenegro, and P. Costa. Development and validation of a weigh-in-motion methodology for railway tracks. *Sensors*, vol. 22, n. 5, 2022.
[4] R. Pimentel, D. Ribeiro, L. Matos, A. Mosleh, and R. Calçada. Bridge weigh-in-motion system for the identification of train loads using fiber-optic technology. *Structures*, vol. 30, pp. 1056–1070, 2021.
[5] N. Bosso, A. Gugliotta, and N. Zampieri. Wheel flat detection algorithm for onboard diagnostic. Measurement, vol. 123, pp. 193–202, 2018.
[6] A. Cavuto, M. Martarelli, G. Pandarese, G. Revel, and E. Tomasini. Train wheel diagnostics by laser ultrasonics. *Measurement*, vol. 80, pp. 99–107, 2016.
[7] A. Amini, M. Entezami, and M. Papaelias. Onboard detection of railway axle bearing defects using envelope analysis of high frequency acoustic emission signals. *Case Studies in Nondestructive Testing and Evaluation*, vol. 6, pp. 8–16, 2016a.
[8] Z. Zhang, M. Entezami, E. Stewart, and C. Roberts. Enhanced fault diagnosis of roller bearing elements using a combination of empirical mode decomposition and minimum entropy deconvolution. *Proceedings of the Institution of Mechanical Engineers, Part C: Journal of Mechanical Engineering Science*, vol. 231, n. 4, pp. 655–671, 2017.
[9] A. Meixedo, A. Gonçalves, R. Calçada, J. Gabriel, H. Fonseca, and R. Martins. Weighing in motion and wheel defect detection of rolling stock. In *2015 3rd Experiment International Conference (exp.at'15)*, pp. 86–90, 2015.
[10] A. Amini, M. Entezami, Z. Huang, H. Rowshandel, and M. Papaelias. Wayside detection of faults in railway axle bearings using time spectral kurtosis analysis on high-frequency acoustic emission signals. *Advances in Mechanical Engineering*, vol. 8, n. 11, pp. 1687814016676000, 2016b.
[11] A. Colaço, P. A. Costa, and D. P. Connolly. The influence of train properties on railway ground vibrations. *Structure and Infrastructure Engineering*, vol. 12, n. 5, pp. 517–534, 2016.
[12] A. Mosleh, A. Meixedo, P. Costa, and R. Calçada. Trackside monitoring solution for weighing in motion of rolling stock. In *Proceedings of the TESTE2019—2nd Conference on Testing and Experimentations in Civil Engineering*, pp. 347–356, Porto, Portugal, 2019.
[13] A. Mosleh, P. A. Costa, and R. Calçada. A new strategy to estimate static loads for the dynamic weighing in motion of railway vehicles. *Proceedings of the Institution of Mechanical Engineers, Part F: Journal of Rail and Rapid Transit*, vol. 234, n. 2, pp. 183–200, 2020a.
[14] A. Mosleh, P. A. Costa, and R. Calçada. Development of a low-cost trackside system for weighing in motion and wheel defects detection. *The International Journal of Railway Research*, vol. 7, n. 1, 2020b.
[15] G. Kouroussis, D. Kinet, V. Moeyaert, J. Dupuy, and C. Caucheteur. Railway structure monitoring solutions using fibre bragg grating sensors. *International Journal of Rail Transportation*, vol. 4, n. 3, pp. 135–150, 2016.
[16] G. Alexandrou, G. Kouroussis, and O. Verlinden. A comprehensive prediction model for vehicle/track/soil dynamic response due to wheel flats. *Proceedings of the Institution of Mechanical Engineers, Part F: Journal of Rail and Rapid Transit*, vol. 230, n. 4, pp. 1088–1104, 2016.
[17] A. Mosleh, P. A. Montenegro, P. A. Costa, and R. Calçada. Railway vehicle wheel flat detection with multiple records using spectral kurtosis analysis. *Applied Sciences*, vol. 11, n. 9, 2021a.
[18] A. Mosleh, P. A. Montenegro, P. A. Costa, and R. Calçada. An approach for wheel flat detection of railway train wheels using envelope spectrum analysis. *Structure and Infrastructure Engineering*, vol. 17, n. 12, pp. 1710–1729, 2021b.
[19] A. Mosleh, A. Meixedo, D. Ribeiro, P. A. Montenegro, and R. Calçada. Early wheel flat detection: an automatic data-driven wavelet-based approach for railways. *Vehicle System Dynamics*, vol. 61, n. 6, pp. 1644–1673, 2023.
[20] R. Wang, D. Crosbee, A. Beven, Z. Wang, and D. Zhen. Vibration-based detection of wheel flat on a high-speed train. In A. Ball, L. Gelman, and B. K. N. Rao, eds, *Advances in Asset Management and Condition Monitoring*, pp. 159–169, Cham. Springer International Publishing, 2020.
[21] X. Xu, J. Liu, S. Sun, and W. Xie. Detection method for polygonalization of wheel treads based on dynamic response. In *Proceedings of the 2020 2nd International Conference on Robotics Systems and Vehicle Technology, RSVT '20*, pp. 16–20, New York, NY, USA. Association for Computing Machinery, 2021.
[22] L. Fang, S. Li, W. Dai, Y. Zhang, Z. Xing, and Y. Han. Method of wheel out-of-roundness detection based on povmd and multinuclear ls-svm. In Y. Qin, L. Jia, B. Liu, Z. Liu, L. Diao, and M. An, eds, *Proceedings of the 4th International Conference on Electrical and Information Technologies for Rail Transportation (EITRT) 2019*, pp. 19–27, Singapore. Springer Singapore, 2020.
[23] T. Hasan. Complex demodulation: Some theory and applications. In *Time Series in the Frequency Domain*, volume 3 of *Handbook of Statistics*, pp. 125–156. Elsevier, 1983.
[24] J. Antoni. Fast computation of the kurtogram for the detection of transient faults. *Mechanical Systems and Signal Processing*, vol. 21, n. 1, pp. 108–124, 2007.
[25] V. Gonçalves, A. Mosleh, C. Vale, and P. A. Montenegro. Wheel out-of-roundness detection using an envelope spectrum analysis. *Sensors*, vol. 23, n. 4, 2023.
[26] MATLAB® version: 9.4.0.813654 (R2018a), Natick, Massachusetts, U.S.A.: The MathWorks Inc.; 2018.
[27] G. Tao, Z. Wen, X. Liang, D. Ren, and X. Jin. An investigation into the mechanism of the out-of-round wheels of metro train and its mitigation measures. *Vehicle System Dynamics*, vol. 57, n. 1, pp. 1–16, 2019.
[28] A. Johansson and C. Andersson. Out-of-round railway wheels—a study of wheel polygonalization through simulation of three-dimensional wheel–rail interaction and wear. *Vehicle System Dynamics*, vol. 43, n. 8, pp. 539–559, 2005.

[29] ANSYS® Academic Research Mechanical Release 19.2, Canonsburg, Pennsylvania, U.S.A.: ANSYS Inc.; 2018.
[30] R. H. Fries and B. M. Coffey. A State-Space Approach to the Synthesis of Random Vertical and Crosslevel Rail Irregularities. *Journal of Dynamic Systems, Measurement, and Control*, vol. 112, n. 1, pp. 83–87, 1990.
[31] A. Hamid and T. Yang. Analytical description of track-geometry variations, 1982.
[32] S. Neves, P. A. Montenegro, A. Azevedo, and R. Calçada. A direct method for analyzing the nonlinear vehicle–structure interaction. *Engineering Structures*, vol. 69, pp. 83–89, 2014.
[33] P. A. Montenegro, S. G. Neves, A. F. Azevedo, and R. Calçada. A nonlinear vehicle-structure interaction methodology with wheel-rail detachment and reattachment. In *ECCOMAS Thematic Conference – COMPDYN 2013: 4th International Conference on Computational Methods in Structural Dynamics and Earthquake Engineering, Proceedings - An IACM Special Interest Conference*, Kos Island, Greece, 2013.
[34] P. A. Montenegro, S. Neves, R. Calçada, M. Tanabe, and M. Sogabe. Wheel–rail contact formulation for analyzing the lateral train–structure dynamic interaction. *Computers Structures*, vol. 152, pp. 200–214, 2015.
[35] J. Kalker, of T. H. D. F. Technical Mathematics, and Informatics. *Book of Tables for the Hertzian Creep-force Law*. Reports of the Faculty of Technical Mathematics and Informatics. Faculty of Technical Mathematics and Informatics, Delft University of Technology, 1996.